J. Fluid Mech. (1996), *vol.* 308, *pp.* 97–110

Symmetrical flow past an accelerated circular cylinder

By H. M. BADR†, S. C. R. DENNIS AND S. KOCABIYIK‡

Department of Applied Mathematics, University of Western Ontario, London, Ontario, N6A 5B7, Canada

(Received 17 September 1993 and in revised form 15 August 1995)

The development of the two-dimensional flow of a viscous incompressible fluid around a circular cylinder which suddenly starts to move with the velocity $U = U_0+U_1t+U_2t^2$ is studied. Equations for the flow in terms of the stream function and vorticity in boundary-layer coordinates are presented. A perturbation series solution for small times is developed. The flow for longer times is computed numerically using an accurate implicit time-integration procedure. The numerical method is checked for small times by comparison with the results of the analytical solution. Reynolds numbers R in the range 200 to 10^4 (based on the diameter of the cylinder) are considered. One particularly interesting result is that for certain values of U_1 and U_2 at $R = 500$ and $R = 10^3$ it is found that two co-rotating vortices and three co-rotating vortices develop with time in each half of the wake in the two respective cases.

1. Introduction

In the present paper we study the two-dimensional flow generated by an infinitely long circular cylinder of radius a which moves with velocity $U = U_0 + U_1t + U_2t^2$ at right angles to its axis. The motion is assumed to be governed by the Navier–Stokes equations for an incompressible fluid and the flow is laminar. There are three basic parameters in the problem. One is the Reynolds number R, defined by $R = 2aU_0/\nu$, where U_0 is the initial velocity of the cylinder which is assumed to be non-zero and ν is the coefficient of kinematic viscosity of the fluid. The other parameters are $\alpha = aU_1/U_0^2$ and $\beta = a^2U_2/U_0^3$ in which the acceleration of the cylinder enters.

Much of the work done prior to this work dealt with the case of a uniformly accelerated cylinder ($U_0 = U_2 = 0$) using boundary-layer theory. In this case the Reynolds number is based on U_1. Solutions have been given for the functional coefficients of powers of the time in a series expansion using analytical methods. The leading term is valid for all values of the Reynolds number R; subsequent terms in the expansion are valid in the case $R \to \infty$. The first work was by Blasius (1908). Three approximations to the initial flow were obtained for this case of infinite R. The theory was extended to finite values of R for the case of a uniformly accelerated

† Permanent address: Mechanical Engineering Department, King Fahd University of Petroleum and Minerals, Dhahran, Saudi Arabia.

‡ Present address: Department of Applied Mathematics, University of Manitoba, Winnipeg R3T 2N2 Manitoba.

start by Collins & Dennis (1974). These extensions were based on the full Navier–Stokes equations rather than the boundary-layer equations. In their work methods of expansion in powers of the time and also methods of numerical integration were employed. These methods were a direct extension of those which were used by Collins & Dennis (1973*a*,*b*); both were later applied in the analysis of Badr & Dennis (1985) to other problems concerned with the initial (two-dimensional) motion of circular cylinders.

One of the objects of the present paper is to give some of the details of the expansion of the solution in powers of the time when the external flow has the given form $U = U_0 + U_1 t + U_2 t^2$. The essential point here is that this expansion gives the exact solution for small times which may be used to check the initial flow details in numerous cases of interest, especially at high Reynolds numbers, where it is difficult to compute the early flow unless boundary-layer coordinates are employed. For example, by making $U_1 = 0$ and an appropriate choice of U_2, we can obtain the initial motion for the case of an oscillating flow in which $U = U_0 \cos(\alpha t) \sim U_0(1-\alpha^2 t^2/2)$. In fact, our expansion procedure may be adapted to determine the early-time solutions in many cases of this problem, e.g. high Reynolds number perturbations to the boundary-layer solutions of Riley (1965), Stuart (1966), Davidson & Riley (1972), Vasantha & Riley (1988). Our methods constitute fairly logical developments of the earlier work of Wang (1965,1968). We shall not, however, consider the oscillating case in detail here. This will be the subject of a further investigation in which comparisons will be made with the recent numerical work of Justesen (1991) and the experimental studies of Williamson (1985) and Tatsuno & Bearman (1990).

We shall also give a numerical treatment of the problem when $U = U_0 + U_1 t + U_2 t^2$ which is satisfactory both initially when boundary-layer theory applies, and also at later times, when recirculation has started and the boundary layer thickens. The numerical method of solution employs boundary-layer variables but without making any approximation to the Navier–Stokes equations. It adopts basically the same type of solution structure as that used by Badr & Dennis (1985). The accuracy of the numerical scheme has been verified by comparing the results with those obtained from the analytical solution at small times and the equations are integrated to later times using an implicit Crank–Nicolson method. The present numerical method can be used to integrate the equations of motion particularly well for high Reynolds numbers because of the employment of the boundary-layer coordinates.

The fully numerical method of solution has been carried out for $R = 200$, 500, 10^3, 10^4 when $\alpha = 0$ and for $\beta = 0.01$, 0.05, 0.1, 0.25. The cases $R = 500$, $\alpha = 0$, $\beta = 0.02$ and $R = 10^3$, $\alpha = 0.05$, $\beta = 0.01$ have also been considered. In all the cases it is found that a pair of secondary vortices is formed at the cylinder surface after a certain time, but that these do not grow substantially with time, although they are more pronounced when $R = 10^3$. On the other hand, a quite new phenomenon occurs for sufficiently large time when $R = 500$, $\alpha = 0$, $\beta = 0.02$ and $R = 10^3$, $\alpha = 0.05$, $\beta = 0.01$. In the first case each part of the symmetrical wake divides into two co-rotating vortices, whereas in the second case each part of the symmetrical wake divides into three co-rotating vortices. In view of the fact that the vortices are co-rotating, this could possibly indicate instability in the wake, although this might be suppressed in the present calculations by the fact that the flow is required to remain symmetrical about the centreline, which has been assumed throughout.

2. Governing equations and method of analysis

A reference frame moving with the cylinder is adopted. Modified polar coordinates (ξ, θ) are used, where $\xi = \log(r/a)$, with the centre of the cylinder as the origin. At time $t = 0$, the cylinder starts to move in the direction $\theta = 0$ with the velocity $U = U_0 + U_1 t + U_2 t^2$, where t is the time. If ψ^* and ζ^* are the stream function and vorticity associated with the motion, we introduce the dimensionless functions ψ and ζ defined by the equations

$$\psi^* = Ua\psi, \quad \zeta^* = -U\zeta/a.$$

The dimensionless radial and transverse components of velocity (u, v) obtained by dividing the corresponding dimensional components by the initial velocity U_0 of the cylinder are then given by

$$u = \mathrm{e}^{-\xi}\frac{\partial \psi}{\partial \theta}, \qquad v = -\mathrm{e}^{-\xi}\frac{\partial \psi}{\partial \xi}, \tag{2.1}$$

and the function ζ is defined by

$$\zeta = \mathrm{e}^{-\xi}\left(\frac{\partial u}{\partial \theta} - \frac{\partial v}{\partial \xi} - v\right). \tag{2.2}$$

Here ψ and ζ satisfy the equations

$$\mathrm{e}^{2\xi}\frac{\partial \zeta}{\partial \tau} = \frac{2}{R}\left(\frac{\partial^2 \zeta}{\partial \xi^2} + \frac{\partial^2 \zeta}{\partial \theta^2}\right) - \frac{\partial \psi}{\partial \theta}\frac{\partial \zeta}{\partial \xi} + \frac{\partial \psi}{\partial \xi}\frac{\partial \zeta}{\partial \theta}, \tag{2.3}$$

$$\frac{\partial^2 \psi}{\partial \xi^2} + \frac{\partial^2 \psi}{\partial \theta^2} = \mathrm{e}^{2\xi}\zeta, \tag{2.4}$$

where τ is defined by $\tau = U_0 t/a$.

Equations (2.3) and (2.4) are those considered by Collins & Dennis (1973*a*,*b*) in the case of sudden translation ($U \neq 0, U_1 = U_2 = 0$) of a circular cylinder without acceleration. Here the acceleration of the fluid enters through the parameters $\alpha = aU_1/U_0^2$ and $\beta = a^2 U_2/U_0^3$ in the boundary conditions, which may be stated as

$$\psi = \frac{\partial \psi}{\partial \xi} = 0 \qquad \text{when} \qquad \xi = 0, \tag{2.5}$$

$$\mathrm{e}^{-\xi}\frac{\partial \psi}{\partial \xi} \to (1 + \alpha\tau + \beta\tau^2)\sin\theta, \quad \mathrm{e}^{-\xi}\frac{\partial \psi}{\partial \theta} \to (1 + \alpha\tau + \beta\tau^2)\cos\theta \quad \text{as} \quad \xi \to \infty. \tag{2.6}$$

The last conditions correspond to an accelerated stream relative to the cylinder at large distances from it. The set of conditions (2.5) and (2.6) must be satisfied for all $\tau > 0$ and for all θ such that $0 \leqslant \theta \leqslant \pi$, and moreover, the flow will be assumed to remain symmetrical about the direction of the motion. Then both functions ψ and ζ are anti-symmetrical about $\theta = 0$ and $\theta = \pi$ and, in particular,

$$\psi(\xi, \theta) = \zeta(\xi, \theta) = 0 \qquad \text{when} \qquad \theta = 0, \qquad \theta = \pi. \tag{2.7}$$

In the present analysis the calculations are carried out on the basis of the method of solution adopted by Collins & Dennis (1973*a*,*b*) in which the functions ψ and ζ were expressed in the form of the series

$$\psi(\xi, \theta, \tau) = \sum_{n=1}^{\infty} f_n(\xi, \tau)\sin n\theta, \tag{2.8}$$

$$\zeta(\xi,\theta,\tau)=\sum_{n=1}^{\infty} g_n(\xi,\tau)\sin n\theta, \tag{2.9}$$

to determine the initial flow in the boundary layer mainly by analytical methods for small values of τ. The equations governing the functions in (2.8) and (2.9) can be obtained by substitution in (2.3) and (2.4). It is found from (2.4) that

$$\frac{\partial^2 f_n}{\partial\xi^2}-n^2 f_n=\mathrm{e}^{2\xi}g_n. \tag{2.10}$$

Equation (2.3) then becomes

$$\mathrm{e}^{2\xi}\frac{\partial g_n}{\partial\tau}=\frac{2}{R}\frac{\partial^2 g_n}{\partial\xi^2}+nf_{2n}\frac{\partial g_n}{\partial\xi}+\left(\frac{1}{2}n\frac{\partial f_{2n}}{\partial\xi}-\frac{2}{R}n^2\right)g_n+S_n, \tag{2.11}$$

where

$$S_n=\frac{1}{2}\sum_{\substack{m=1\\ m\neq n}}^{\infty}\left[((m+n)f_{m+n}-jf_j)\frac{\partial g_m}{\partial\xi}+m\left(\frac{\partial f_{m+n}}{\partial\xi}-\mathrm{sgn}(m-n)\frac{\partial f_j}{\partial\xi}\right]g_m. \right. \tag{2.12}$$

Here $j=|\,m-n\,|$ and $\mathrm{sgn}(m-n)$ denotes the sign of $m-n$, with $\mathrm{sgn}(0)=0$. The set of equations (2.10) and (2.11) hold for all positive integer values of n.

Boundary conditions follow from (2.5) and (2.6). From (2.5)

$$f_n=\frac{\partial f_n}{\partial\xi}=0 \quad \text{when} \quad \xi=0, \tag{2.13}$$

for all n. As a consequence of the condition (2.6) we must also have that, for all n,

$$g_n(\xi,\tau)\to 0 \quad \text{as} \quad \xi\to\infty. \tag{2.14}$$

Finally, the conditions (2.6) imply that

$$\mathrm{e}^{-\xi}\frac{\partial f_n}{\partial\xi}\to(1+\alpha\tau+\beta\tau^2)\delta_{n,1}, \quad \mathrm{e}^{-\xi}\frac{\partial f_n}{\partial\theta}\to(1+\alpha\tau+\beta\tau^2)\delta_{n,1} \quad \text{as} \quad \xi\to\infty, \tag{2.15}$$

where $\delta_{m,n}$ is the Kronecker delta symbol defined by

$$\delta_{m,n}=1 \quad \text{if} \quad m=n, \quad \delta_{m,n}=0 \quad \text{if} \quad m\neq n.$$

If we multiply (2.10) by $\mathrm{e}^{-n\xi}$ and integrate from $\xi=0$ to $\xi=\infty$, we may deduce, using (2.13) and (2.15) that

$$\int_0^{\infty}\mathrm{e}^{(2-n)\xi}g_n(\xi,\tau)\mathrm{d}\xi=2(1+\alpha\tau+\beta\tau^2)\delta_{n,1}, \tag{2.16}$$

where $\delta_{n,1}$ has the significance in (2.15). It can be shown that the conditions (2.13), (2.14) and (2.16) are sufficient to solve the problem, and that, if they are satisfied and $g_n(\xi,\tau)$ is assumed to be such that $\mathrm{e}^{2\xi}g_n(\xi,\tau)$ is bounded for all n as $\xi\to\infty$, then the flow is automatically adjusted to satisfy the external stream condition (2.6). The functions $g_n(\xi,\tau)$ can be verified to satisfy the necessary condition *a posteriori*.

Equations (2.10) and (2.11) determine the development of the flow at some time after the impulsive start, but in the initial stages of the motion the boundary-layer coordinate x can be introduced by the transformation

$$\xi=kx, \quad k=2(2\tau/R)^{1/2}. \tag{2.17}$$

This is employed to transform all the appropriate equations together with the scalings of variables

$$f_n = kF_n, \quad g_n = \frac{G_n}{k}. \tag{2.18}$$

Equation (2.10) then becomes

$$\frac{\partial^2 F_n}{\partial x^2} - n^2k^2F_n = \mathrm{e}^{2kx}G_n, \tag{2.19}$$

while equation (2.11) becomes

$$\begin{aligned} 4\tau\frac{\partial G_n}{\partial \tau} = \mathrm{e}^{-2kx}\frac{\partial^2 G_n}{\partial x^2} + \left(2x + 4n\tau F_n e^{-2kx}\right)\frac{\partial G_n}{\partial x} \\ + \left[2 + \mathrm{e}^{-2kx}\left(2n\tau\frac{\partial F_{2n}}{\partial x} - n^2k^2\right)\right]G_n + 4\tau\mathrm{e}^{-2kx}S_n^*, \end{aligned} \tag{2.20}$$

where S_n^* is S_n with f_n replaced by F_n, g_n replaced by G_n and ξ replaced by x.

The boundary conditions simply become

$$F_n = \frac{\partial F_n}{\partial x} = 0 \qquad \text{when} \qquad x = 0, \tag{2.21}$$

and

$$\int_0^\infty \mathrm{e}^{(2-n)kx}G_n(x,\tau)\mathrm{d}x = 2(1 + \alpha\tau + \beta\tau^2)\delta_{n,1}. \tag{2.22}$$

The solution at the start of the motion is found by putting $\tau = k = 0$ in (2.19) and (2.20), and in the condition (2.22). Equations (2.20) become

$$\frac{\partial^2 G_n}{\partial x^2} + 2x\frac{\partial G_n}{\partial x} + 2G_n = 0. \tag{2.23}$$

The solutions of these satisfying (2.22) are

$$G_n(x,0) = 4\pi^{-1/2}\delta_{n,1}\mathrm{e}^{-x^2}, \tag{2.24}$$

which yields the expression

$$\zeta(x,\theta,0) = 4\pi^{-1/2}\mathrm{e}^{-x^2}\sin\theta; \tag{2.25}$$

the corresponding solutions to (2.19) obtained using (2.24) are easily found as

$$F_n = 2[x\mathrm{erf}x - \pi^{-1/2}(1 - \mathrm{e}^{-x^2})]\delta_{n,1}, \tag{2.26}$$

which gives the initial expression for $\psi(x,\theta,0)$.

From the initial expressions (2.24) and (2.26) we may now build up a perturbation solution in powers of τ following Collins & Dennis (1973*a*). The expansions for the stream function and vorticity can be made in terms of both k and τ. First we may expand ψ and ζ in the form

$$\psi = \psi_0 + k\psi_1 + k^2\psi_2 + \ldots, \quad \zeta = \zeta_0 + k\zeta_1 + k^2\zeta_2 + \ldots, \tag{2.27}$$

where $\psi_m \equiv \psi_m(x,\theta,\tau)$, $\zeta_m \equiv \zeta_m(x,\theta,\tau)$. Then each ψ_m, ζ_m is expanded as a series of powers of τ in the form

$$\psi_m(x,\theta,\tau) = \sum_{n=0}^{\infty}\psi_{mn}(x,\theta)\tau^n, \quad \zeta_m(x,\theta,\tau) = \sum_{n=0}^{\infty}\zeta_{mn}(x,\theta)\tau^n, \tag{2.28}$$

where each of the coefficients ψ_{mn}, ζ_{mn} consists of combinations of functions of x with periodic functions of θ. The process of derivation of these coefficients follows very closely the procedures described by Collins & Dennis (1973*a*). The differential equations for the functions $\psi_{mn}(x,\theta),\zeta_{mn}(x,\theta)$ and the boundary conditions satisfied by these functions can easily be found. Each of these functions can be expressed as a finite set of Fourier-sine components in the coordinate θ with coefficients which are functions of the variable x. The series (2.27) are thus expressed in periodic terms in θ with coefficients depending on x,τ and k. On expansion in powers of τ and k and equating to zero each coefficient of $k^m\tau^n$, we get the conditions which the Fourier-sine components must satisfy. As a result of determining seven composite functions $\zeta_{mn}(x,\theta)$ in the series (2.28) when $\alpha = 0$ and $\beta = O(1)$, we obtain an expression for the vorticity of the form

$$\zeta(x,\theta,\tau) \sim \zeta_{00} + \tau\zeta_{01} + \tau^2\zeta_{02} + k\left(\zeta_{10} + \tau\zeta_{11} + \tau^2\zeta_{12}\right) + k^2\left(\zeta_{20} + O(\tau)\right), \tag{2.29}$$

which is valid for small τ and large R. For our present purpose we shall only give the expression obtained for the surface vorticity. The expression (2.29) obtained by analytical means gives sufficient information to check the numerical solutions which are obtained by numerical integration of (2.19) and (2.20) subject to the conditions (2.21) and (2.22). In particular, we find for the surface vorticity

$$\begin{aligned}\zeta(0,\theta,\tau) \sim\ & \left(4\pi^{-1/2} + k - \tfrac{1}{4}\pi^{-1/2}k^2\right)\sin\theta - \tau\left[\tfrac{4}{3}\pi^{-3/2}(3\pi+4)\right. \\ & \left.-\tfrac{1}{120}\pi^{-1}\left(15\pi\left[96\times 2^{1/2} - 77\right] - 304\right)\right]\sin 2\theta + \tau^2\left[\left(\tfrac{1}{135}\pi^{-2}\left[1440\pi^2(1+\beta)\right.\right.\right. \\ & \left.\left.\left.-(3402\times 3^{1/2} - 2196)\pi - 2816\right] + [1.60170 + \beta]k\right)\sin\theta\right. \\ & \left.+\left(\tfrac{1}{135}\pi^{-5/2}\left[180\pi^2 - \left(1458\times 3^{1/2} - 1404\right)\pi + 256\right] + 4.92853k\right)\sin 3\theta\right],\end{aligned} \tag{2.30}$$

when $\alpha = 0$ and $\beta = O(1)$. Some further results derived from these solutions will be given subsequently.

As we mentioned previously, the initial solution given by (2.24) and (2.26) forms the starting point of the analytical solution (2.29) for the vorticity in powers of τ, and it likewise forms the starting point of the numerical solution of (2.19) and (2.20). In the initial stages only a very few terms of the series (2.8) and (2.9) are required to describe the flow, but more terms become necessary as time-dependent integrations proceed. This is exactly analogous to the case of expansion in powers of τ, where each new power of τ introduces higher periodic terms in the expansions (2.8) and (2.9). However, the advantage of the present method is that the numerical integrations can be carried on long after the series in powers of τ ceases to be valid; further, the method is not restricted to high values of R.

3. Numerical integration procedure

In order to calculate the flow for any Reynolds number and large enough time, the numerical method of integration given by Badr & Dennis (1985) may be used. The solution is started in the boundary-layer variables by integrating (2.19) and (2.20) using (2.24) and (2.26) as initial conditions and (2.21) and (2.22) as boundary conditions. An implicit method of integration of Crank–Nicolson type is used, and a given approximation is obtained by truncating the series (2.8) and (2.9). This is done

by setting to zero all functions $F_n(x,\tau)$ and $G_n(x,\tau)$ for $n > n_0$, where n_0 is an integer defining the order of truncation. Thus in practice $2n_0$ functions are determined from (2.19) and (2.20).

The essential details of the procedure have been given by Badr & Dennis (1985). Only a few functions $F_n(x,\tau)$ and $G_n(x,\tau)$ are needed to describe the motion for small τ in view of the initial structure given by (2.24) and (2.26). More functions are added as integration proceeds and the parameter n_0 actually refers to the maximum number of terms used in each of the series (2.8) and (2.9) during the integration. Checks were made for each R at several typical values of τ to ensure that n_0 was large enough. This was done by increasing n_0 and observing that the solution did not change appreciably. It is also necessary to use a small time step for small τ. The reason is that the expansions of $F_n(x,\tau)$ and $G_n(x,\tau)$ in powers of τ depend also upon integer powers of k, thus all derivatives with respect to τ of terms involving odd powers of k are eventually singular at $\tau = 0$ after a certain stage, provided R is finite. The problem does not arise in the boundary-layer case, where $k = 0$. However, when $k \neq 0$ care must be taken to minimize the effect of singularities in derivatives at $\tau = 0$ and the only effective way of dealing with this is to take very small time steps so that the effect of higher derivatives tends to be smoothed out by the small $\Delta\tau$.

For the cases of finite R considered the integrations were all started by taking 10 time steps $\Delta\tau = 10^{-4}$. The time step was then increased to $\Delta\tau = 10^{-3}$ for the next 10 steps and then to $\Delta\tau = 10^{-2}$ for the next 10. Finally $\Delta\tau = 0.025$ was taken for the rest of the solution. The grid size in the x-direction was taken as $\Delta x = 0.05$ and the maximum value of x was $x_M = 8$. The values of grid sizes were to some extent chosen to be comparable with those used by Badr & Dennis (1985), since these were found to be satisfactory and were checked carefully. A few comparable checks on different grids were made at one or two values of τ during the present calculations. Moreover, the solutions obtained by fully numerical means are compared with the results obtained using expansions in powers of τ; these comparisons indicate that the solutions are quite accurate. Finally, we may note that the numerical method described may be used to continue the solution for increasing τ in terms of the physical coordinate ξ when the boundary layer thickens. The same methods may be used to integrate (2.10) and (2.11) subject to the boundary conditions in terms of these coordinates. However in the present paper only cases for which $R \geqslant 200$ are presented and it is possible to work in terms of the boundary-layer coordinate x over the entire range of τ considered.

Since the time step $\Delta\tau$ near $\tau = 0$ is obviously significant we have carried out some tests on one of the cases for which detailed results will be presented in the next section, namely $R = 500$, $\alpha = 0$, $\beta = 0.02$. For the grid size $\Delta x = 0.05$ the results of varying the time step during the solution near $\tau = 0$ was carefully studied, keeping $\Delta x = 0.05$. Several runs were made with different values of $\Delta\tau$ and found to be completely consistent. For example, with $\Delta\tau = 0.0125$, the total drag coefficient C_D at $\tau = 1.0$ was 1.0648 compared with 1.0646 when $\Delta\tau = 0.05$. This is a comparison of a global property, of course, but comparisons of solution details were similar. At $\tau = 5.0$, C_D=3.4608 when $\Delta\tau = 0.0125$ compared with $C_D = 3.4607$ when $\Delta\tau = 0.05$. The change in space step tends to be more significant. For example, when $\tau = 0.05$, $C_D = 1.0600$ at $\tau = 1.0$ when $\Delta x = 0.1$ compared with $C_D = 1.0646$ when $\Delta x = 0.05$. However, by careful study of the effect of changes in both $\Delta\tau$ and Δx, the results presented are thought to be reliable.

β	0.01	0.05	0.1	0.25	0.5
T	0.3203	0.3236	0.3279	0.3426	0.3732

TABLE 1. Approximations of the time, T, when the recirculation begins for the boundary-layer case ($k = 0$ or $R = \infty$) when $\alpha = 0$.

4. Results and comparisons

One of the interesting physical features of the flow is the determination of the time at which the fluid first starts to form a recirculating region at the rear of the cylinder. It occurs at a time $\tau = T$, say, defined by the condition $\partial\zeta/\partial\theta = 0$ for $x = 0$, $\theta = 0$. From the expansion (2.29) in powers of k and τ we can obtain various approximations to T by investigating the roots of the equation

$$\sum_{m=0}^{m_0}\sum_{n=0}^{n_0} k^m T^n (\partial\zeta_{mn}/\partial\theta)_{x=\theta=0} = 0 \tag{4.1}$$

when $\alpha = 0$ and $\beta = O(1)$. Here m_0 and n_0 correspond to the total number of terms taken in the series (2.27) and (2.28) for $\zeta(x, \theta, \tau)$. The boundary-layer ($R = \infty$) case corresponds to $m_0 = 0$ and successive approximations to T are obtained by taking increasing values of n_0. If we take $n_0 = 1$ in the boundary-layer case we obtain

$$T = 3\pi[2(3\pi + 4)]^{-1} = 0.3510217 \tag{4.2}$$

which is in agreement with the Blasius approximation in the case of the impulsively started translating circular cylinder. The second approximation ($n_0 = 2$) gives the time T as the positive root of

$$\frac{1}{135}\pi^{-2}\left[4\left(45\pi^2(11 + 8\beta) - \pi\left(19443^{1/2} - 2196\right) - 1602\right) - 512\right] T^2 - \tfrac{8}{3}\pi^{-1}(3\pi + 4)T + 4 = 0. \tag{4.3}$$

This yields the value $T = 0.319504$ when $\beta = 0$ which is in agreement with the approximation given by Collins & Dennis (1973*a*) in the case of an impulsively started translating circular cylinder. Approximations corresponding to various values of β have been calculated and these are shown in table 1. An investigation of the variation of T with R and β has been carried out by finding the appropriate root of the equation

$$\begin{aligned}\frac{1}{135}\pi^{-2}\ &\left(\left[180(11 + 8\beta)\pi^2 - \left(7776 \times 3^{1/2} - 6408\right)\pi - 1602\right] - 2048\right) T^2 \\ &- \left(\frac{2T}{R}\pi\right)^{1/2}\left[\frac{1}{3360}\pi^{-2}\left(105\left(64\beta + 7008 \times 2^{1/2} + 4509\right)\pi^2 - 1514731.4\pi^{3/2}\right.\right. \\ &+ \left(379904 \times 2^{1/2} + 771120 \times 3^{1/2} - 1270928\right)\pi - 141312\Big) T^2 \\ &\left.\left. - \tfrac{1}{30}\left(1440 \times 2^{1/2} - 1150\pi^{-1}\right) T - 2\right] - \tfrac{8}{3}\pi^{-1}(3\pi + 4)T + 4 = 0\end{aligned} \tag{4.4}$$

incorporating all the terms in (4.1), when $m_0 = 1$ and $n_0 = 2$, which have been calculated. The results are shown in table 2. The results of table 2 show that R has a stronger influence on the time T when the first recirculation begins at lower β than

R/β	0.01	0.05	0.1
200	0.5952	0.6692	–
500	0.4172	0.4263	0.4322
10^3	0.3792	0.3854	0.3396
10^4	0.3357	0.3396	0.3447

TABLE 2. The effect of the first two boundary-layer correction terms, on the time, T, when the first recirculation begins for the case $\alpha = 0$.

R/β	0.01	0.05	0.1
200	0.4468	0.4523	0.4593
500	0.3948	0.3984	0.4029
10^3	0.3724	0.3754	0.3791
10^4	0.3372	0.3392	0.3418

TABLE 3. Calculated values of the time, T, when the recirculation begins from the numerical solution for the case $\alpha = 0$.

at higher β in the case $\alpha = 0$. It is clear that numerical methods must be used to give accurate values for lower values of R. The range of R for which these results are valid is not known but some evidence is available from the results of the numerical calculations which are given in table 3.

A dimensionless drag coefficient C_D is defined by $C_D = D/\rho U^2 a$ where D is the total drag on the cylinder. It may be expressed as

$$C_D = \frac{4}{R}\int_0^{\pi}\left(\zeta - \frac{\partial\zeta}{\partial\zeta}\right)_{\xi=0}\sin\theta\,\mathrm{d}\theta, \tag{4.5}$$

in which the first term in the integral gives the friction drag coefficient C_f and the second the pressure drag coefficient C_p, where $C_D = C_f + C_p$. Both of these coefficients can be calculated as series in powers of τ and k from the present results. It is found, for the terms calculated, that

$$\begin{aligned} C_f = \pi(2R\tau)^{-1/2}\big[&4\pi^{-1/2} + \tfrac{1}{135}\pi^{-5/2}\left(2\left[360\pi^2(2\beta+2) - 9\pi\left(189\times 3^{1/2} - 122\right) - 1408\right]\right)\tau^2 \\ &+k - \left(\tfrac{1}{4}\pi^{-1/2}\right)k^2 - \tfrac{1}{26880}\pi^{-2}\left(105\pi^2\left(128\alpha^2 - 7292\times 2^{1/2} + 4785\right) + 1451520\beta\pi^{3/2}\right. \\ &\left.+\pi\left(610304\times 2^{1/2} + 1533168\times 3^{1/2} - 2300144\right) - 362496\right)k\tau^2 + O(\tau^3)\big], \end{aligned} \tag{4.6}$$

$$\begin{aligned} C_p = \frac{\pi}{4\tau}\big[&16\beta\tau^2 + 4\pi^{-1/2}k + k^2 - \tfrac{1}{15120}\pi^{-5/2}\left(80640\pi^2\left(\alpha^2 - 12\,2^{1/2} + 6\right)\right. \\ &+4354560\beta\pi^{3/2} - \pi\left(430080\times 2^{1/2} - 381024\times 3^{1/2} - 345408\right) \\ &\left.+315392\right).k\tau^2 + O(\tau^3)\big] \end{aligned} \tag{4.7}$$

Finally, we may also obtain an exact expression for the pressure coefficient p_0^*:

$$p_0^* = \frac{p_0(\theta,\tau) - p_0(\pi,\tau)}{(\frac{1}{2})\rho U^2} = -\frac{4}{R}\int_{\theta}^{\pi}\left(\frac{\partial\zeta}{\partial\zeta}\right)_{\xi=0}\mathrm{d}\theta. \tag{4.8}$$

This coefficient p_0^* measures the change in dimensionless pressure over the surface of the cylinder and the subscript zero denotes a value at the surface $\xi = 0$. It may be

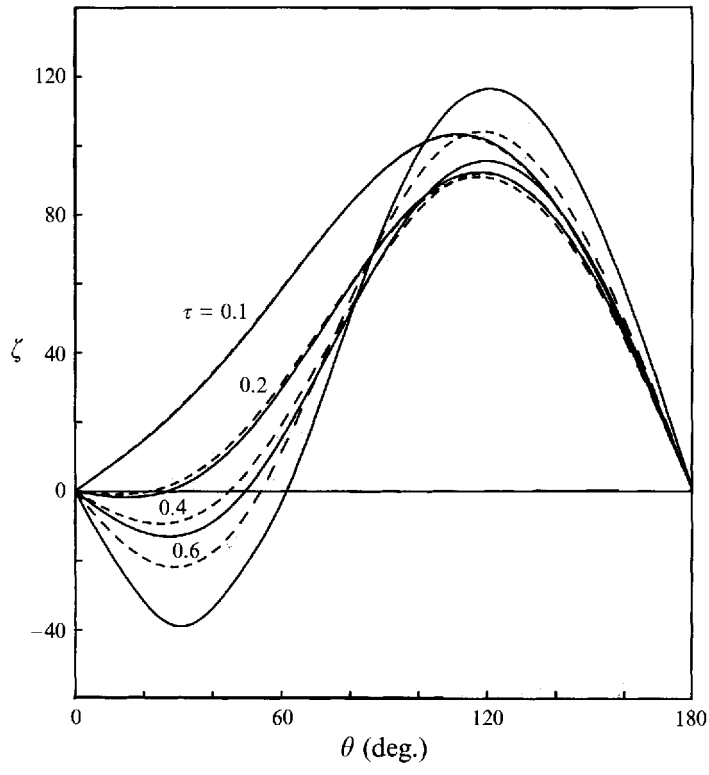

FIGURE 1. Comparison of the vorticity distribution over the surface of the cylinder at $R = 10^4$, $\alpha = 0$, $\beta = 0.25$: —, numerical solution; - - -, analytical solution.

shown that the expression for p_0^* found from the second equation of (2.27) using (4.8) is

$$p_0^* = \frac{1}{2\tau}\left[4(\cos 2\theta - 1)\tau - \left(16\beta(\cos\theta + 1) + \tfrac{1}{3}\pi^{-3/2}\left[\pi\left(7 - 2^{1/2} - 60\right) - 16\right]\right.\right.$$
$$\times(\cos 2\theta - 1))\,\tau^2 - 4\pi^{-1/2}(\cos\theta + 1)k - [(6.018\beta + 4.59154)(\cos\theta + 1)$$
$$\left.\left. + (366.6926\beta + 41.5813)(\cos 3\theta + 1)]\,k\tau^2\right]. \qquad (4.9)$$

These analytical expressions will now be used to check the results of the numerical integrations at small values of τ. A comparison between the results for the surface vorticity obtained from the numerical solutions at small values of τ and obtained from (2.30) when $\alpha = 0$ and $\beta = 0.25$ is given in figure 1. The agreement is found to be satisfactory for small enough times. Calculated results exhibited in figure 2 for C_D obtained from (4.6) and (4.7) again compare satisfactorily with the results derived from the numerical procedure described in the last section at small values of τ. In figure 3, the pressure variation around the cylinder surface according to the present numerical calculation at $R = 10^4$ when $\alpha = 0$, $\beta = 0.25$ is compared with analytical result (4.9) at $\tau = 0.1, 0.2, 0.4$ and $\tau = 0.6$.

The time development of flow patterns for the cases $R = 500$, $\alpha = 0$, $\beta = 0.02$ and $R = 10^3$, $\alpha = 0.05$, $\beta = 0.01$ at values of τ over the range $\tau = 1.0$ to 18.0 are shown in figures 4 and 5. The growth of the length of the vortex pair obtained from the numerical solutions is given in figure 6, which shows that with the increase of time the vortices are increasing in a roughly linear manner once recirculation has

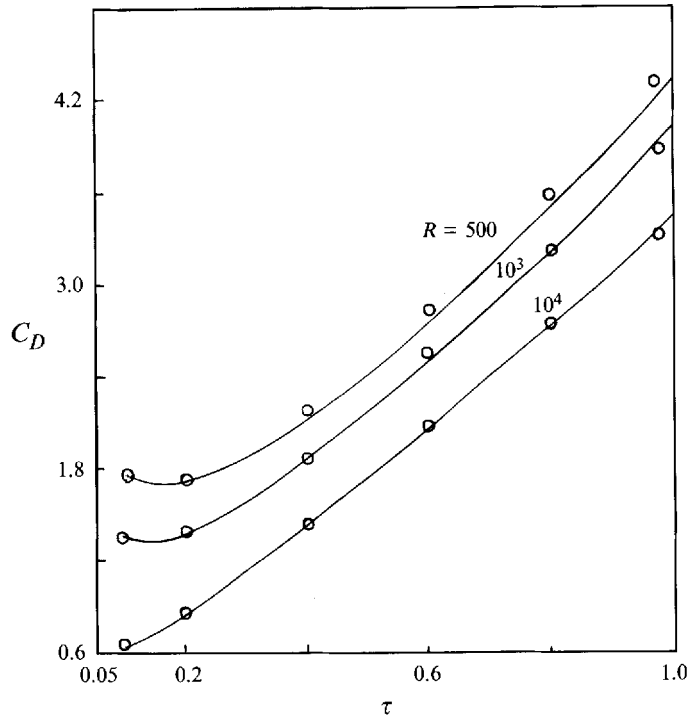

FIGURE 2. Variation of the drag coefficient C_D with τ at $\alpha = 0$, $\beta = 0.25$: ——, numerical solution; ○, analytical solution.

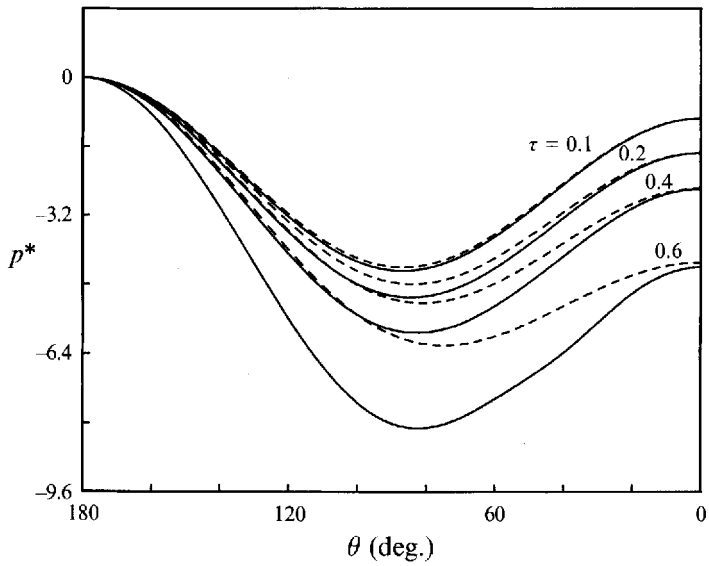

FIGURE 3. Comparison of the variation of the pressure coefficient over the surface of the cylinder at $R = 10^4$, $\alpha = 0$, $\beta = 0.25$: ——, numerical solution; - - -, analytical solution.

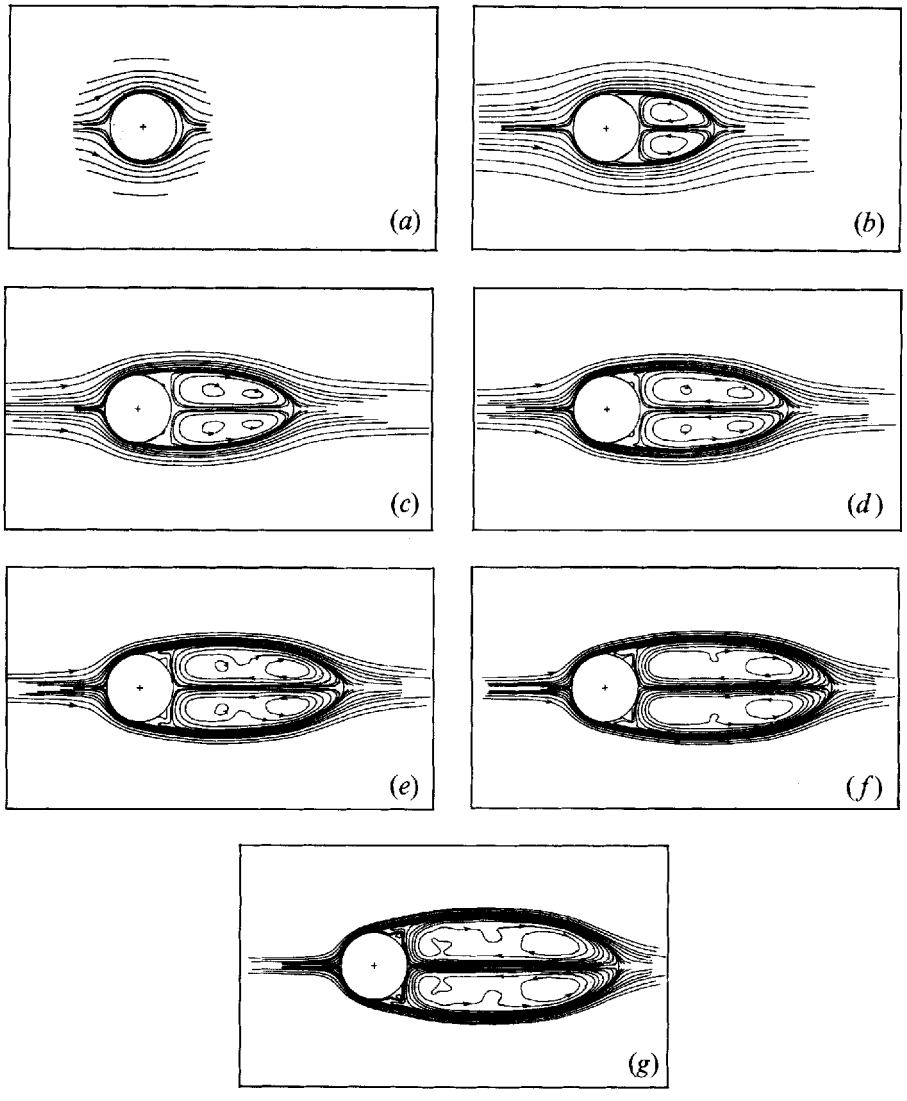

FIGURE 4. Instantaneous streamlines of the flow for $R = 500$, $\alpha = 0$, $\beta = 0.02$ at various times: (a) $\tau = 1.0$, (b) 6.0, (c) 10.0, (d) 12.0, (e) 14.0, (f) 16.0, (g) 18.0.

established itself. Here $L(\tau)$ is the dimensionless length of the recirculation region measured in radii along the downstream axis of symmetry from the rearmost point of the cylinder.

In both cases a pair of secondary vortices appears after a certain time. They become more pronounced in the $R = 10^3$ case, but do not seem to grow for later times. However, the development of the flow for later times is quite different in the two cases. Thus, in the $R = 500$ case at $\tau = 10.0$ each vortex in the pair breaks into two co-rotating vortices, whereas in the $R = 10^3$ case at $\tau = 14.0$ each vortex breaks into three co-rotating vortices, a phenomenon which does not seem to have been observed previously in flows of this kind. The cause of the difference of the flow development in the two cases is not clear, but the acceleration of the fluid in the external flow becomes much greater at larger times in the $R = 500$ case.

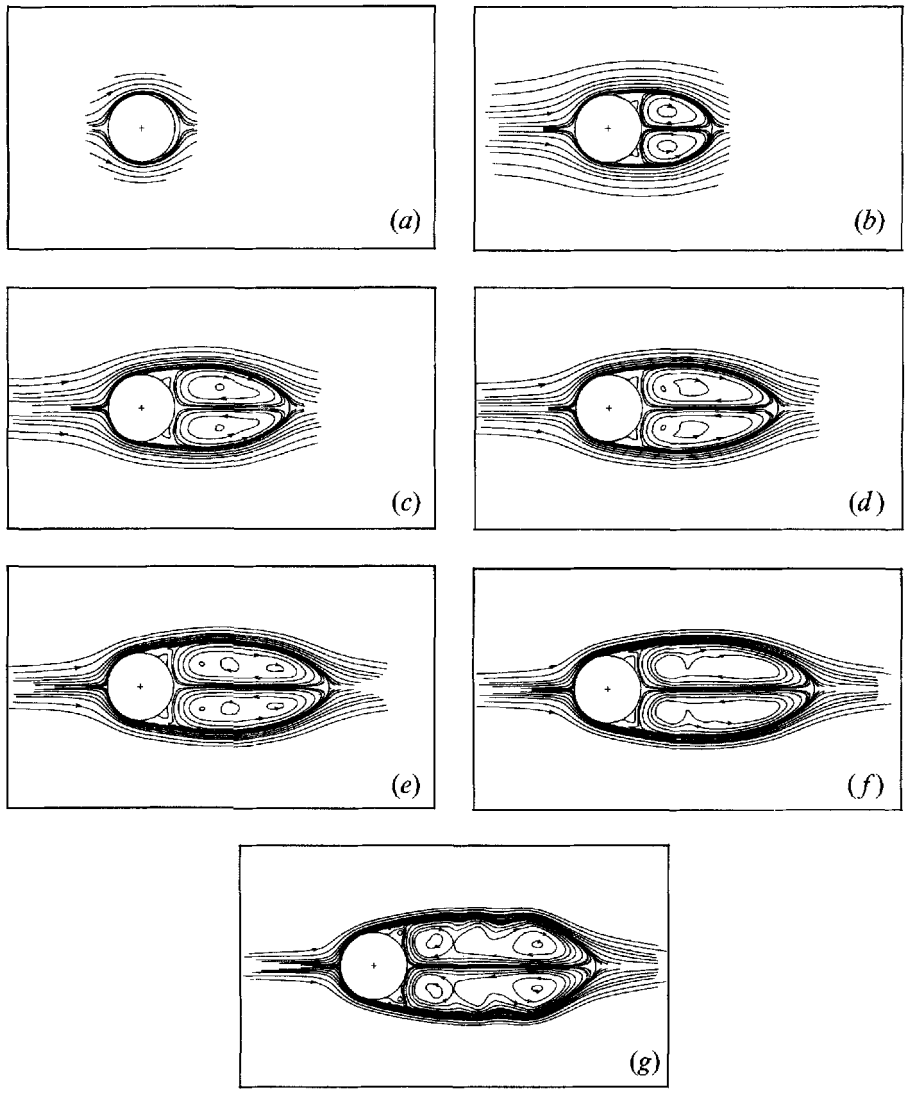

FIGURE 5. Instantaneous streamlines of the flow for $R = 10^3$, $\alpha = 0.05$, $\beta = 0.01$ at various times: (*a*) $\tau = 1.0$, (*b*) 6.0, (*c*) 10.0, (*d*) 12.0, (*e*) 14.0, (*f*) 16.0, (*g*) 18.0.

In any case the situation of two co-rotating vortices would seem to be potentially unstable.

5. Conclusions

In the present paper we have considered the flow due to an accelerated circular cylinder and found analytical expressions which describe the initial flow. These expressions are used to check the initial details of a fully numerical study of the problem which is extended well beyond the range of applicability of the analytical solutions. The numerical work has been continued sufficiently far in time to reveal some new and interesting features in the wake, in which the flow breaks down into two or three co-rotating vortices, depending upon the Reynolds number.

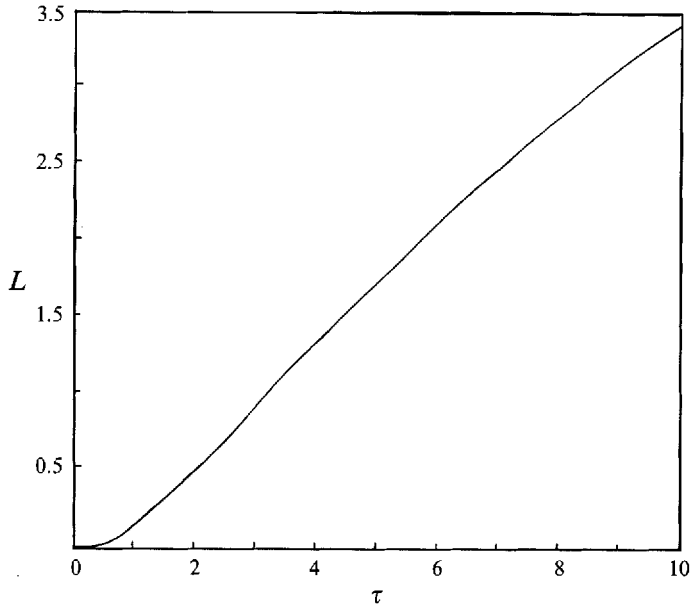

FIGURE 6. Variation of the wake length as a function of τ for $R = 10^3$, $\alpha = 0.05$, $\beta = 0.01$.

The support of the Natural Sciences and Engineering Research Council of Canada for this investigation is gratefully acknowledged. We also acknowledge the interest and support of the King Fahd University of Petroleum and Minerals, Dhahran.

REFERENCES

BADR, H. M. & DENNIS, S. C. R. 1985 Time-dependent viscous flow past an impulsively started rotating and translating circular cylinder. *J. Fluid Mech.* **158**, 447–488.

BLASIUS, H. 1908 Grenzschichten in Flüssigkeiten mit kleiner Reibung. *Z. Angew. Math. Phys.* **56**, 1–37. (Translated as 'The boundary layers in fluids with little friction'. *Tech. Mem. Nat. Adv. Comm. Aero., WA No.* 1256.)

COLLINS, W. M. & DENNIS, S. C. R. 1973*a* The initial flow past an impulsively started circular cylinder. *Q. J. Mech. Appl. Maths* **26**, 53–75.

COLLINS, W. M. & DENNIS, S. C. R. 1973*b* Flow past an impulsively started circular cylinder. *J. Fluid Mech.* **60**, 105–127.

COLLINS, W. M. & DENNIS, S. C. R. 1974 Symmetrical flow past a uniformly accelerated circular cylinder. *J. Fluid Mech.* **65**, 461–480.

DAVIDSON, B. J. & RILEY, N. 1972 Jets induced by oscillatory motion. *J. Fluid Mech.* **53**, 287–303.

JUSTESEN, P. 1991 A numerical study of oscillating flow around a circular cylinder. *J. Fluid Mech.* **222**, 157–196.

RILEY, N. 1965 Oscillating viscous flows. *Mathematika.* **12**, 161–175.

STUART, J. T. 1966 Double boundary layers in oscillatory viscous flows. *J. Fluid Mech.* **24**, 673–687.

TATSUNO, M. & BEARMAN, P. W. 1990 A visual study of the flow around an oscillating circular cylinder at low Keulegan–Carpenter numbers and low Stokes numbers. *J. Fluid Mech.* **211**, 157–182.

VASANTHA, R. & RILEY, N. 1988 On the initiation of jets in oscillatory viscous flows. *Proc. R. Soc. Lond.* A **419**, 363–378.

WANG, C.-Y. 1965 The resistance on a circular cylinder in an oscillating stream. *Q. Appl. Maths* **23**, 305–312.

WANG, C.-Y. 1968 On high-frequency oscillatory viscous flows. *J. Fluid Mech.* **312**, 55–68.

WILLIAMSON, C. H. K. 1985 Sinusoidal flow relative to circular cylinders. *J. Fluid Mech.* **155**, 141–174.